

## Spectral Energy Balance of Breaking Waves within the Surf Zone\*

T. H. C. HERBERS AND N. R. RUSSNOGLE

*Department of Oceanography, Naval Postgraduate School, Monterey, California*

STEVE ELGAR

*Applied Ocean Physics and Engineering, Woods Hole Oceanographic Institution, Woods Hole, Massachusetts*

(Manuscript received 7 December 1998, in final form 14 December 1999)

### ABSTRACT

The spectral energy balance of ocean surface waves breaking on a natural beach is examined with field observations from a cross-shore array of pressure sensors deployed between the shoreline and the outer edge of the surf zone near Duck, North Carolina. Cross-shore gradients in wave energy flux were estimated from spectral changes observed between closely spaced sensors. Direct, empirical estimates of nonlinear energy exchanges between different frequency components of the wave spectrum were obtained from observed bispectra using Boussinesq theory for near-resonant triad wave-wave interactions. The large decrease in energy flux observed across the surf zone in the energetic part of the wave spectrum is balanced closely by the estimated nonlinear energy transfers from the spectral peak to higher frequencies. In the high-frequency tail of the spectrum, observed energy flux gradients are small and do not balance the nonlinear energy transfers. This analysis indicates that the observed decay of wave spectra in the surf zone is primarily the result of nonlinear energy transfers to higher frequencies, and that dissipation occurs in the high-frequency tail of the spectrum where energy levels are relatively low.

### 1. Introduction

Nonlinear wave-wave interactions play a central role in the shoaling evolution of surface gravity waves on beaches. In shallow water ( $kh \ll 1$ , with  $k$  the wave-number and  $h$  the water depth) near-resonant interactions between three wave components with frequencies  $f_1$ ,  $f_2$ , and  $f_3$ , that obey the interaction rule  $f_1 + f_2 - f_3 = 0$ , can cause large energy exchanges over distances of only a few wavelengths (Freilich and Guza 1984). These triad interactions transfer energy from the dominant waves to higher and lower frequencies, broadening and phase coupling the wave spectrum, and causing the dramatic transformation from smooth sinusoidal wave shapes in deep water to the characteristic steep, pitched-forward crests of near breaking waves (Elgar and Guza 1985a).

The nonlinear shoaling transformation of waves on beaches is described well by Boussinesq-type equations

for weakly nonlinear, weakly dispersive waves (Peregrine 1967). Freilich and Guza (1984) solved the coupled evolution equations for the amplitudes and phases of a discrete Fourier expansion of waves propagating over a gently sloping beach. Predictions of spectral statistics were obtained by averaging the results of many model realizations with random phase initial conditions. Herbers and Burton (1997) developed an alternative statistically averaged model, based on a third-order weakly non-Gaussian closure, that describes the shoaling evolution of the spectrum and bispectrum of random waves. Predictions of both the deterministic and the stochastic formulations of Boussinesq wave shoaling models agree well with field observations of the evolution of wave spectra on beaches (e.g., Freilich and Guza 1984; Elgar and Guza 1985b; Norheim et al. 1998).

Boussinesq models have been extended into the surf zone by including a heuristic dissipation term in the shoaling evolution equations (Mase and Kirby 1992; Kaihatu and Kirby 1995; Eldeberky and Battjes 1996; Chen et al. 1997). The parameterizations used in these models are somewhat arbitrary because the spectral characteristics of dissipation rates in the surf zone are not known. Eldeberky and Battjes (1996) used a frequency-independent dissipation term that reduces spectral levels uniformly in proportion to the energy at each frequency  $f$ . Based on laboratory measurements, Mase

---

\* Woods Hole Oceanographic Institution Contribution Number 10062.

---

Corresponding author address: Dr. Thomas H. C. Herbers, Department of Oceanography, Code OC/He, Naval Postgraduate School, Monterey, CA 93943-5122.  
E-mail: herbers@oc.nps.navy.mil

and Kirby (1992) and Kaihatu and Kirby (1995) used a dissipation function that contains a frequency-independent term and a frequency-dependent ( $\propto f^2$ ) term that is weighted toward higher-frequency components of the wave spectrum. Few measurements of the spectral characteristics of surf zone dissipation have been reported. Smith and Vincent (1992) observed the surf zone decay of a mixed swell-sea wave field in a laboratory flume, and showed that the presence of the lower-frequency swell causes a more rapid decay of the higher-frequency sea component. Chen et al. (1997) used Boussinesq model predictions to show that this decay can be explained by large nonlinear energy transfers to other parts of the spectrum. Comparison of Boussinesq model predictions with field observations indicates that nonlinear triad interactions play an important role in the spectral energy balance of a natural surf zone, and suggests that relative dissipation rates of spectral components increase with frequency (Elgar et al. 1997). Based on a detailed analysis of several laboratory and field datasets, Chen et al. (1997) demonstrated that the evolution of wave shapes across the surf zone is predicted more accurately by Boussinesq models with dissipation that increases with frequency than by models using frequency-independent dissipation.

In the present study the spectral energy balance of shoaling and breaking waves is examined in more detail using field observations from a dense cross-shore array of pressure sensors deployed on a sandy ocean beach. Neglecting alongshore depth variations, directional spreading of waves, and wave reflection from shore, the energy transport equation can be expressed as a balance between the cross-shore gradient of the energy flux spectrum  $F_x(f)$ , a nonlinear source term  $S_{nl}(f)$ , and a dissipation term  $S_{ds}(f)$  that accounts for wave breaking-induced energy losses:

$$F_x(f) = S_{nl}(f) + S_{ds}(f). \quad (1)$$

The energy flux spectrum is given by  $F(f) = c_g(f)\rho g E(f)$ , where  $c_g$  is the wave group speed,  $\rho$  is the density of seawater,  $g$  is gravity, and  $E(f)$  is the surface elevation spectrum. In the Boussinesq approximation, energy is transmitted with the shallow water group speed  $c_g = (gh)^{1/2}$ . The energy flux gradient  $F_x(f)$  was evaluated from differences in energy flux measured at adjacent instruments in the cross-shore array.

The nonlinear source term  $S_{nl}(f)$  represents the net transfer of energy to waves with frequency  $f$  through near-resonant triad interactions. The energy transfers are controlled by the phase-relationship between the three interacting components, and thus depend on higher-order statistics of the wave field. A stochastic formulation of the spectrum evolution equation [Eq. (22a) in Herbers and Burton 1997] yields a simple relation between the nonlinear source term  $S_{nl}(f)$  and an integral of the surface elevation bispectrum  $B(f_1, f_2)$

$$S_{nl}(f) = \text{Im} \left\{ \frac{3\pi f}{h} \rho g \left( \int_0^f df' B(f', f - f') - 2 \int_0^\infty df' B(f', f) \right) \right\}, \quad (2)$$

where  $\text{Im}$  indicates the imaginary part. The bispectrum  $B(f_1, f_2)$  describes statistically the phase relationship and energy exchange within the  $(f_1, f_2, f_1 + f_2)$  triad. If  $\text{Im}\{B(f_1, f_2)\}$  is positive, then energy is transferred from the  $f_1$  and  $f_2$  components to the higher-frequency  $f_1 + f_2$  component. For negative  $\text{Im}\{B(f_1, f_2)\}$  the energy transfer reverses and the lower frequency components  $f_1$  and  $f_2$  grow at the expense of the higher-frequency  $f_1 + f_2$  component. The energy transfer vanishes when  $\text{Im}\{B(f_1, f_2)\} = 0$  (e.g., steady wave solutions in uniform depth). The net nonlinear transfer of energy to wave components with frequency  $f$  is obtained by integrating the energy exchanges with all  $(f_1, f_2, f_1 + f_2)$  triads that include a component with frequency  $f$  [Eq. (2)].

The energy flux gradient  $F_x(f)$  and nonlinear source term  $S_{nl}(f)$  were calculated from spectra and bispectra of waves measured in water depths ranging from 5 to 1 m. The field data and analysis are described in section 2. Observations of the energy balance for a range of conditions are presented in section 3. In the surf zone, large negative values of  $F_x(f)$  in the energetic part of the spectrum are shown to be balanced approximately by the estimated  $S_{nl}(f)$ , indicating that the observed decay of spectral levels is primarily the result of large nonlinear energy transfers to higher frequencies where presumably the energy is dissipated. The results are discussed in section 4 and summarized in section 5.

## 2. Field data and analysis

A dense cross-shore transect of 13 pressure sensors was deployed between the shoreline and about 5-m depth (350 m from shore) on a barred ocean beach near Duck, North Carolina (Fig. 1: Elgar et al. 1997). Collocated with each pressure sensor was a sonar altimeter that provided accurate estimates of the vertical elevation of the seafloor. Data were collected nearly continuously (sample frequency 2 Hz) during September and October 1994.

The closely spaced pressure sensors allow for direct estimates of the energy flux gradient term  $F_x(f)$  and the nonlinear source term  $S_{nl}(f)$  in the energy balance equation (1) (normalized by  $\rho g$  hereafter). At all instrument locations the wave spectrum  $E(f)$  and bispectrum  $B(f_1, f_2)$  were estimated from 1-h-long pressure records, neglecting second-order vertical variations of wave properties over the water column (e.g., Peregrine 1967). The spectral and bispectral estimates are based on Fourier transforms of detrended and windowed 256-s-long data segments with 75% overlap. The raw

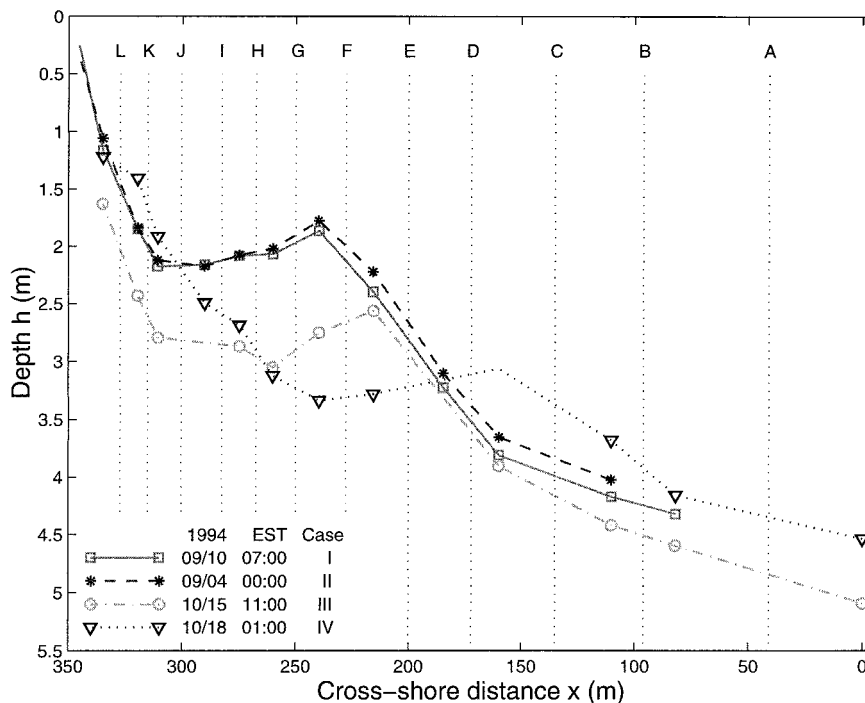


FIG. 1. Depth profiles for each of the four case studies with symbols denoting the cross-shore positions where wave measurements were collected. The vertical dotted lines and letters **A** through **L** indicate the midway points between adjacent instruments where the energy balance [Eq. (1)] was evaluated. The date and start time of each case study is listed in the legend.

spectra and bispectra were ensemble averaged and smoothed to yield final estimates of  $E(f)$  and  $B(f_1, f_2)$  with a frequency resolution of 0.0078 Hz and approximately 60 degrees of freedom.

The energy balance was evaluated at each midway point between adjacent instruments (Fig. 1). The energy flux gradient  $F_x(f)$  was estimated based on a finite difference approximation:

$$F_x(f) = \frac{E_2(f)[gh_2]^{1/2} - E_1(f)[gh_1]^{1/2}}{x_2 - x_1}, \quad (3)$$

where  $x_1, x_2$  ( $>x_1$ ) are the cross-shore positions of a pair of adjacent sensors, and  $h_1, h_2$  and  $E_1(f), E_2(f)$  are the corresponding water depths and spectra. An estimate of the nonlinear source term at the same midway point was obtained through linear interpolation of  $S_{nl}$  estimates at the two adjacent instruments [Eq. (2)]:

$$S_{nl}(f) = \frac{3\pi f}{2} \text{Im} \left\{ \int_0^f df' \left( \frac{B_1(f', f-f')}{h_1} + \frac{B_2(f', f-f')}{h_2} \right) - 2 \int_0^{f_{\max}-f} df' \left( \frac{B_1(f', f)}{h_1} + \frac{B_2(f', f)}{h_2} \right) \right\}, \quad (4)$$

$$0 < f < f_{\max},$$

where  $B_1$  and  $B_2$  are the bispectral estimates at instrument locations  $x_1$  and  $x_2$ , and the cutoff frequency  $f_{\max} = 0.5$  Hz. Only triads with all three frequencies  $f_1, f_2$ , and  $f_1 + f_2$  in the range  $(0, f_{\max})$  contribute to the integrals of Eq. (4). For each of these triads there is an exact balance between the energy lost (gained) by the two lower frequency ( $f_1, f_2$ ) components and the energy gained (lost) by the higher frequency ( $f_1 + f_2$ ) component, and thus  $\int_0^{f_{\max}} df S_{nl}(f)$  is constrained to be equal to zero.

Estimates of  $S_{nl}(f)$  at the dominant wave frequencies (nominally 0.06–0.25 Hz) are insensitive to the high-frequency (0.5 Hz) truncation of Eq. (4), but estimates of nonlinear transfers in the high-frequency tail of the spectrum are not expected to be accurate because interactions that involve a frequency  $>0.5$  Hz are excluded. The neglected hydrodynamic attenuation of short-wavelength components causes additional errors in estimates of  $F_x(f)$  and  $S_{nl}(f)$  at high frequencies.

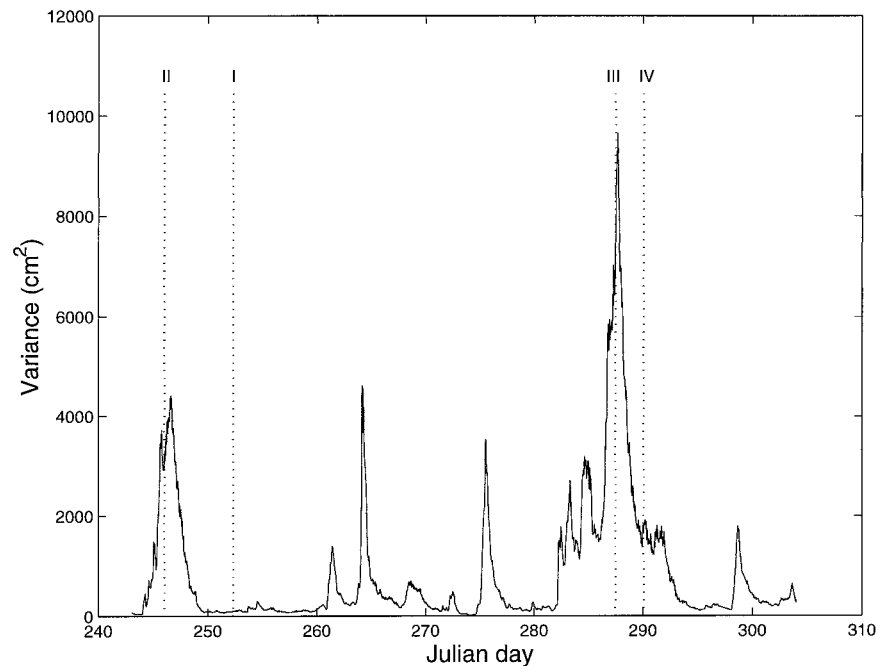


FIG. 2. Hourly estimates of the incident wave variance (in the frequency range 0.05–0.25 Hz) vs time for the two-month data collection period. The variance estimates were obtained from bottom pressure measurements in 8-m depth (instruments deployed and maintained by the U.S. Army Corps of Engineers) using a linear theory depth correction. Dotted vertical lines indicate the four case studies examined in section 3.

Furthermore, the Boussinesq approximation upon which Eq. (4) is based is not accurate in the dispersive high-frequency tail of the spectrum where triad interactions are nonresonant. Other mechanisms (e.g., resonant quartet interactions and turbulence) not considered here may play an important role in the spectral energy balance at high frequencies. The present analysis is focused on the energy balance within the energy containing part of the wave spectrum, where  $F_x$  and  $S_{nl}$  are described accurately by the shallow water Boussinesq approximations (3) and (4).

The two-month observation period spanned a wide range of wave conditions, including two storms with maximum significant wave heights of 2.5 and 3.8 m (Fig. 2) and wide surf zones extending across the entire instrumented transect. Shoaling of nonbreaking waves was observed during many calm periods with significant wave heights as small as 0.2 m. The observations include narrow spectra of remotely generated swell, broad spectra of locally generated seas, and bimodal spectra of mixed swell–sea systems (Elgar et al. 1997). The beach profile during the experiment featured a well-developed sand bar approximately 100 m from shore (Fig. 1). Seaward of the sand bar, the bottom profile was planar with a gentle ( $\sim 1:200$ ) slope. Intense wave breaking often occurred on the shallow ( $h \approx 1.5\text{--}2.0$  m at low tide) crest of the sand bar. Inshore of the bar crest a nearly flat section, 80 m wide, extended to a steep ( $\sim 1:20$ ) beach face. Changes in the bathymetry

were small in the first 1.5 months of the experiment, but during the most severe storm in the middle of October the sand bar moved about 80 m offshore (Fig. 1; Gallagher et al. 1998).

### 3. Observed spectral energy balance

The spectral energy balance in shoaling and breaking waves is illustrated with four case studies that span a wide range of conditions (Fig. 2). For each case, the evolution of the spectrum  $E(f)$  across the beach is shown in Fig. 3, and a representative video image of the sea surface in the array vicinity is shown in Fig. 4. In case I, small amplitude swell propagated across the instrumented transect with little breaking. The evolution of the narrow spectrum shows the expected growth of harmonic peaks. Breaking and associated energy losses occurred primarily on the beach face at the shoreward end of the instrument array (Fig. 4). In both case studies II and III, taken from storms, an irregular surf zone with spilling breakers extended across the entire 350-m-long transect (Fig. 4). The spectra observed in these storms are similar, with a strong, nearly uniform decay of spectral levels across the surf zone (Fig. 3). In case IV, during the waning of the second storm, directionally narrower, moderately energetic swell was observed. This case is characterized by a narrow surf zone confined to the inner part of the instrument array, with intermittent breaking of larger waves farther offshore on the crest of the sand

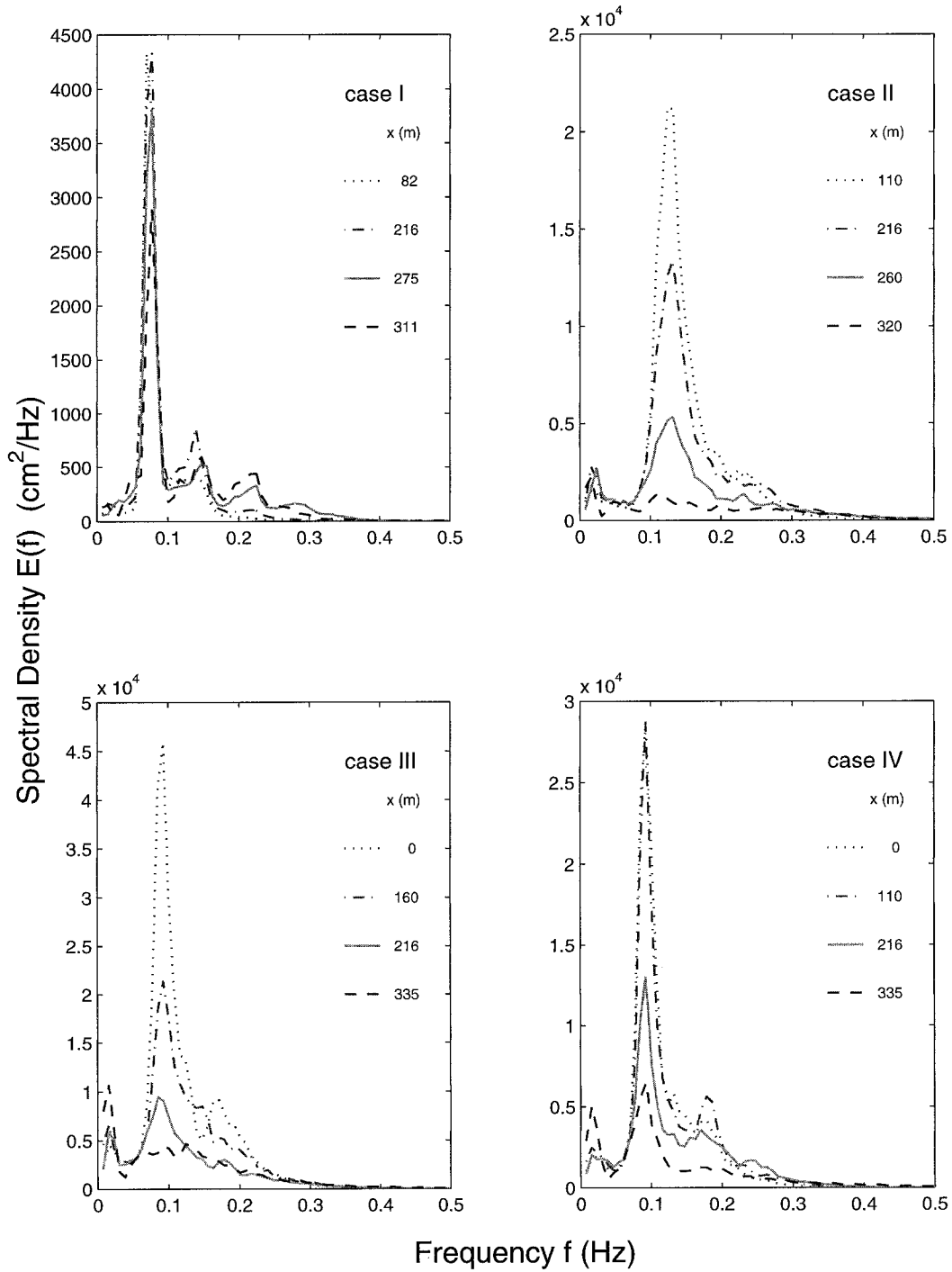


FIG. 3. Spectral density vs frequency for the four case studies. In each case spectra are shown at four measurement locations spanning the cross-shore transect (Fig. 1).

bar (Fig. 4). There was strong decay of both the primary and the second-harmonic spectral peaks in the surf zone, and amplification of lower-frequency infragravity motions.

To examine the role of nonlinear interactions in the spectral evolution observed in these four case studies,

empirical estimates of the nonlinear source term  $S_{nl}(f)$  [Eq. (4)] are compared with estimates of the energy flux gradient  $F_x(f)$  [Eq. (3)] in Figs. 5–8. In all cases (both with nonbreaking and with breaking waves) the integral of  $S_{nl}(f)$  over all frequencies is equal to zero because the nonlinear interactions conserve energy.

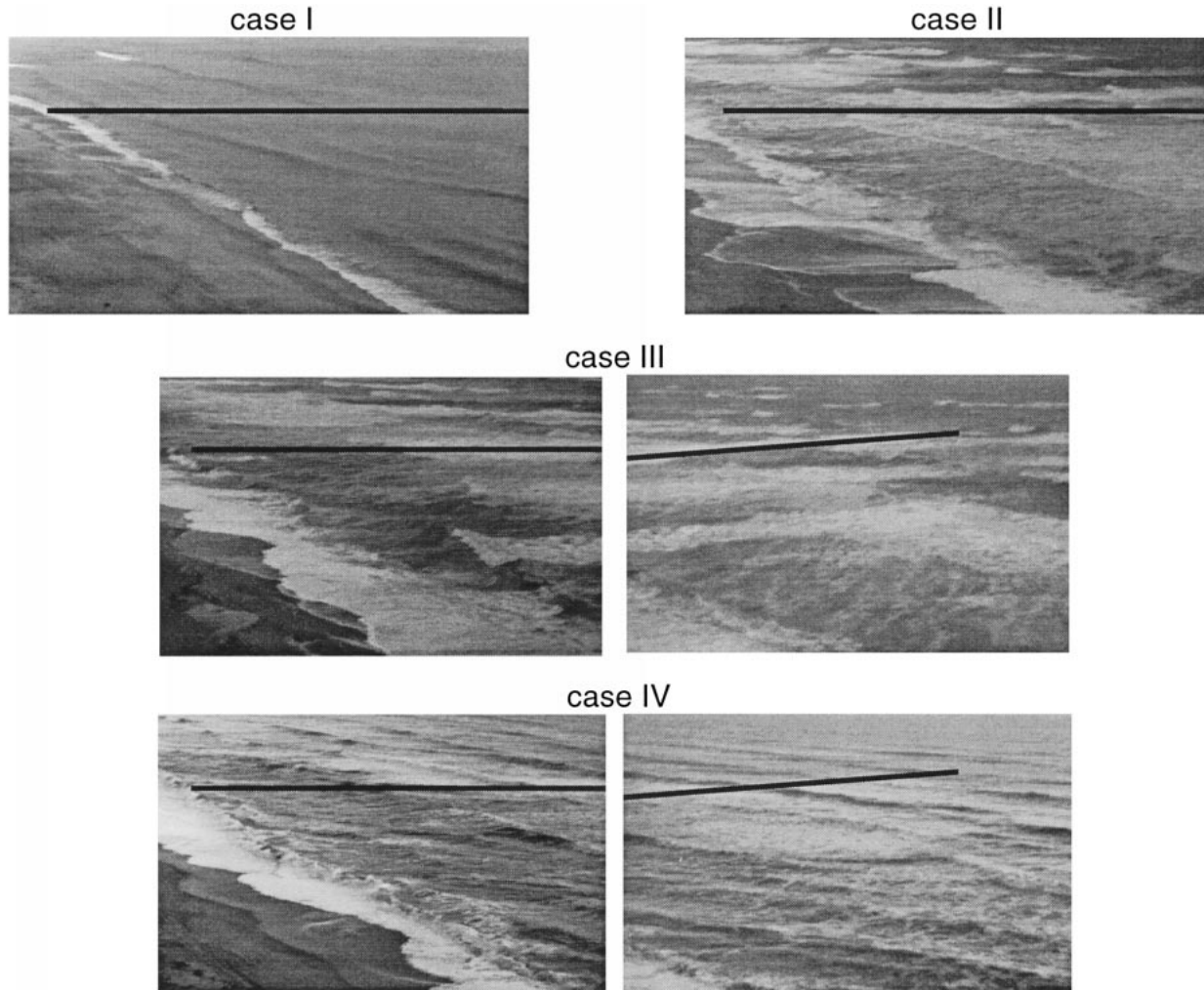


FIG. 4. Photographs of surf zone conditions in the four case studies. The photographs (courtesy of T. C. Lippmann) were obtained with two video cameras mounted on a nearby tower about 50 m above the sea surface. The top, middle-left, and lower-left photographs cover the same area, which includes the inner half of the instrumented transect (solid line). The middle-right and bottom-right photographs are simultaneous, slightly overlapping ( $\sim 20$  m) views of the outer half of the instrumented transect (solid line) in cases III and IV. The outward-looking camera was not operational during cases I and II.

#### a. Case I

In case I with small nonbreaking waves (Fig. 5: the significant wave height in 8-m depth  $H_s = 0.4$  m) the  $S_{nl}(f)$  estimates are negative near the spectral peak frequency ( $f_p = 0.07$  Hz) and positive at higher frequencies. At the deeper locations B–D the negative values of  $S_{nl}$  at  $f_p$  are balanced by positive values at  $2f_p$ . The relatively small nonlinear transfers indicate the weak initial growth of the second-harmonic peak (0.14 Hz) of the spectrum at the expense of the primary peak (0.07 Hz). At location E the  $S_{nl}$  estimate contains an additional positive peak at frequency  $3f_p$  indicating energy transfer to a third harmonic (0.21 Hz). The nonlinear energy transfers increase dramatically as waves propagate over the crest of the sand bar (F–G) and remain strong on the flat section inshore of the bar crest (H–J). The  $S_{nl}$

estimates are similar at locations F–J, with a narrow region of negative values at  $f_p$  balanced by smaller positive values at harmonic frequencies. These nonlinear energy transfers to phase-locked harmonic components cause the familiar shoaling evolution of wave shapes from initial sinusoidal profiles to steep, pitched-forward crests characteristic of nearly breaking waves (e.g., Elgar and Guza 1985a). Small negative values of  $S_{nl}(f)$  at high frequencies at the shallowest stations (e.g.,  $f > 0.25$  Hz, H–J) suggest a slight reversal in energy transfer.

The observed positive values of  $F_x(f)$  at frequencies  $f > 0.1$  Hz agree with the  $S_{nl}(f)$  estimates, confirming that the spectral growth at high frequencies is primarily the result of nonlinear energy transfers, consistent with Boussinesq model results for similar

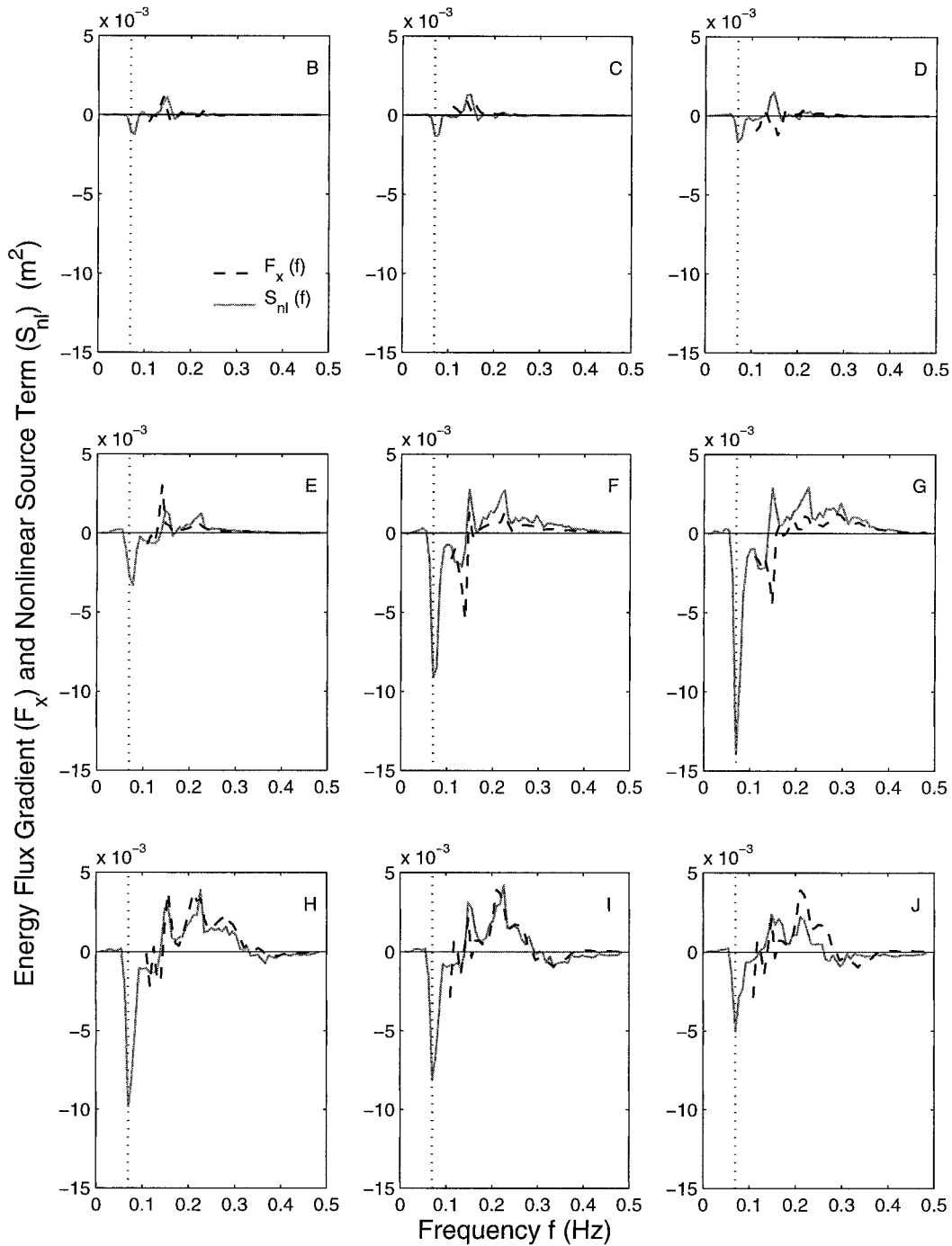


FIG. 5. Comparison of the energy flux gradient  $F_x(f)$  (dashed curve) with the nonlinear source term  $S_{nl}(f)$  (solid curve) observed in case I. The letter in the upper-right corner of each panel denotes the cross-shore position where the energy balance was evaluated (see Fig. 1). The vertical dotted lines indicate the peak frequency  $f_p$  of the incident wave spectrum (observed at the farthest offshore sensor).

conditions (Elgar et al. 1997; Norheim et al. 1998). The observed agreement of  $S_{nl}(f)$  with  $F_x(f)$  estimates in nonbreaking wave conditions with presumably negligible dissipation ( $S_{ds}(f) \approx 0$ ) is not unexpected, but confirms that the new bispectral estimation

procedure yields reasonably accurate estimates of  $S_{nl}(f)$ . Although bispectral estimates based on short data records have considerable statistical uncertainty, the errors in  $S_{nl}(f)$  caused by statistical fluctuations in individual bispectrum estimates are reduced by the

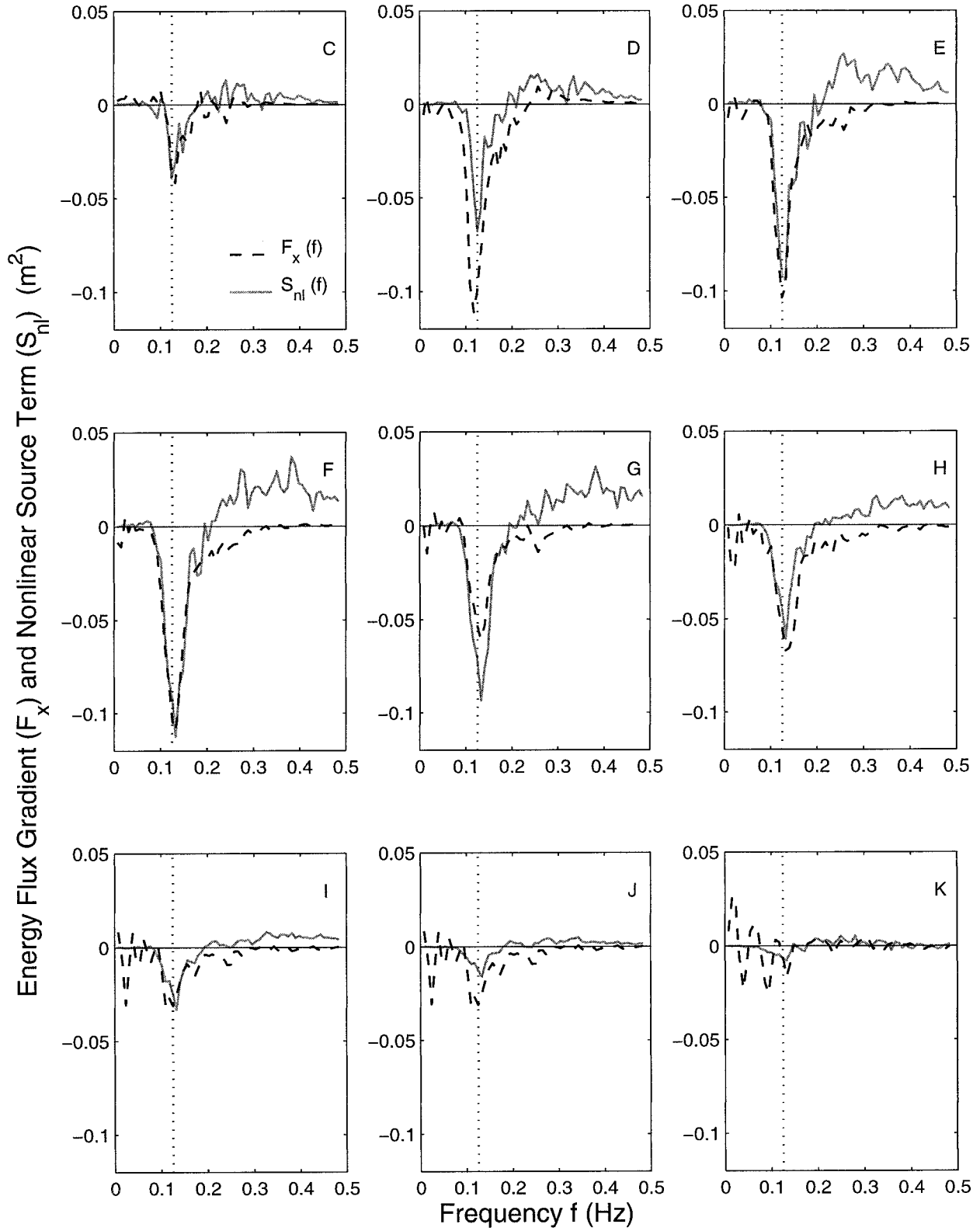


FIG. 6. Comparison of the energy flux gradient  $F_x(f)$  with the nonlinear source term  $S_{nl}(f)$  observed in case II (same format as Fig. 5).

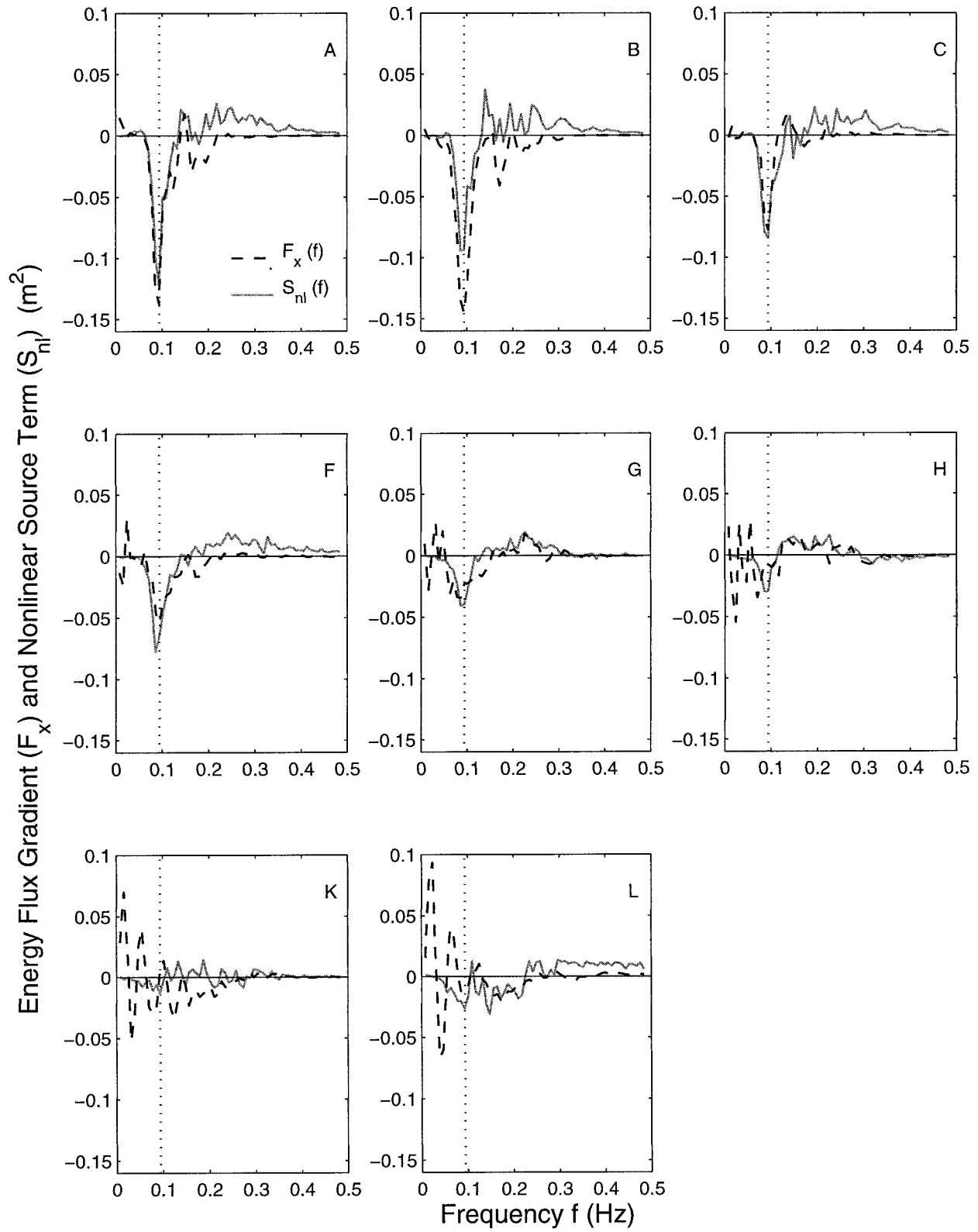


FIG. 7. Comparison of the energy flux gradient  $F_x(f)$  with the nonlinear source term  $S_{nl}(f)$  observed in case III (same format as Fig. 5).

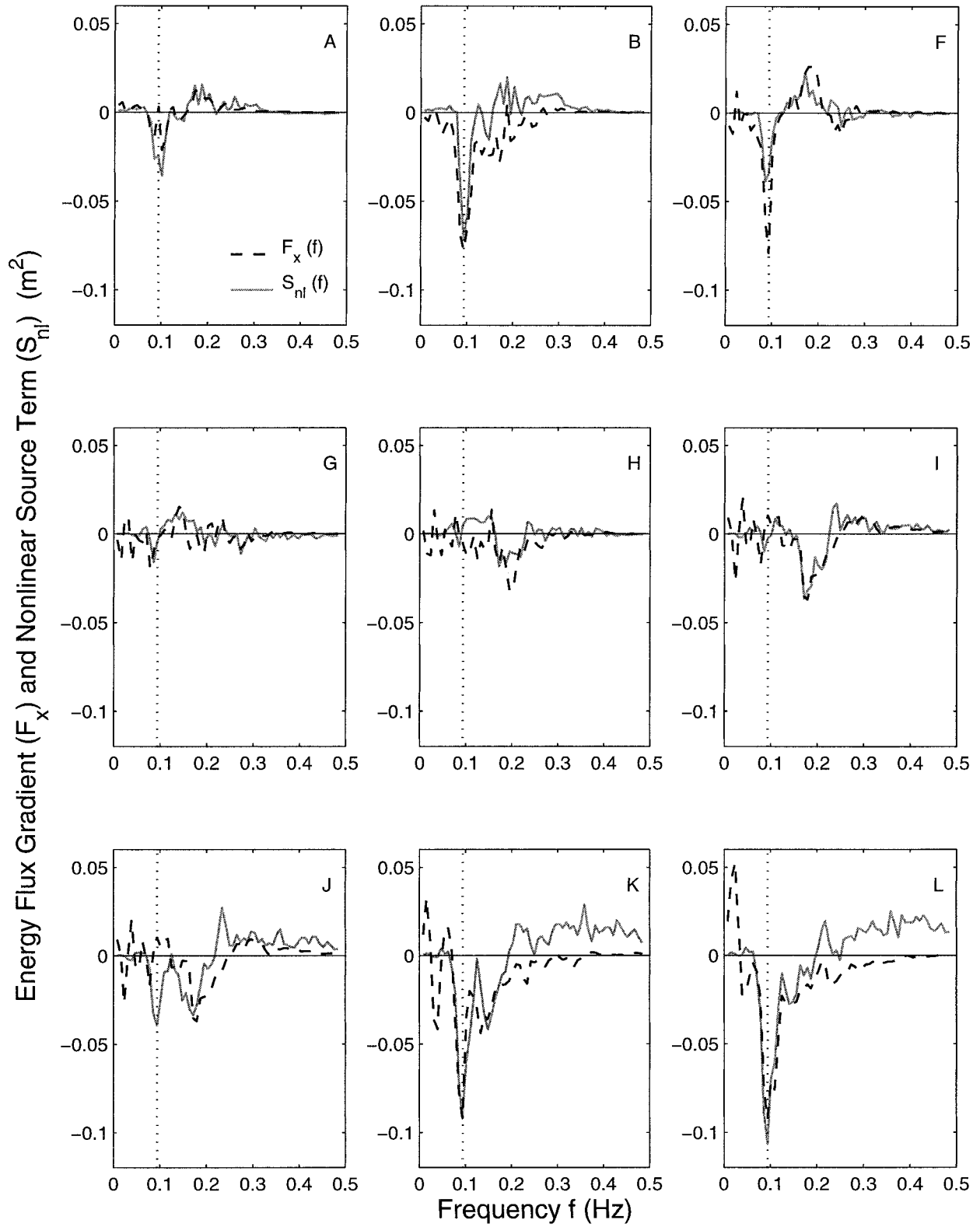


FIG. 8. Comparison of the energy flux gradient  $F_x(f)$  with the nonlinear source term  $S_{nl}(f)$  observed in case IV (same format as Fig. 5).

integration [Eq. (2)] over all triads involving frequency  $f$  (e.g., Herbers et al. 1994).

Estimates of  $F_x(f)$  at lower frequencies ( $f < 0.1$  Hz) are not shown because partial reflection of these components from the steep beach face (Elgar et al. 1994, 1997) contributes significant errors. The  $F_x(f)$  estimates are based on measured potential energy, assuming equipartitioning of potential and kinetic energy, and thus are not accurate in partial standing waves with cross-shore fluctuations (i.e., nodes and antinodes) in the relative contributions of potential and kinetic energy (e.g., Kinsman 1965). No comparisons of  $S_{nl}(f)$  with  $F_x(f)$  are shown at the shallowest stations K and L (Fig. 1) because the more pronounced standing wave patterns at these locations within 35 m of the shoreline strongly affect estimates of spectra and bispectra at all frequencies [see Elgar et al. (1997) and Norheim et al. (1998) for further discussion].

#### b. Case II

Whereas case I and other cases with nonbreaking waves (not shown) validate the procedure to estimate terms in the energy balance equation (1), of greater interest are the remaining cases II–IV with breaking waves because the role of nonlinear triad interactions within the surf zone is not established well. In case II with moderately energetic seas ( $H_s = 2.2$  m,  $f_p = 0.125$  Hz) waves broke across the entire transect. At all cross-shore locations the  $S_{nl}$  estimates are negative near the spectral peak frequency ( $0.1 < f < 0.2$  Hz) and positive at higher frequencies, indicating that energy is transferred primarily from the energetic part of the spectrum to higher frequencies. The nonlinear energy transfers increase from the farthest offshore station in operation during this event (C) to a maximum value on the crest of the sand bar (F), followed by a gradual decrease to small values near the shoreline. The estimated negative energy flux gradients  $F_x$  in the energetic part of the spectrum nearly equal the negative  $S_{nl}$  estimates. The close balance between  $F_x$  and  $S_{nl}$  at all stations indicates that the strong decay of the spectral peak in the surf zone (the peak spectral level is reduced by a factor 20 between the deepest and shallowest sensors, Fig. 3) is caused primarily by nonlinear transfers to higher frequencies rather than by direct dissipation of the incident wave components.

The observed energy flux gradients and nonlinear transfers do not balance at higher frequencies. Whereas  $S_{nl}(f)$  estimates are positive at frequencies greater than about 0.2 Hz (i.e., energy received from the spectral peak), the corresponding  $F_x(f)$  estimates are close to zero. These results suggest that the energy transferred through nonlinear interactions to higher frequencies cannot be absorbed in the high-frequency tail of the spectrum and, presumably is dissipated at the rate it is transferred, qualitatively consistent with the saturation of wave spectra in the surf zone observed by Thornton

(1977, 1979) and with model results by Chen et al. (1997).

At the inner surf zone stations I–K the  $F_x(f)$  estimates have fluctuations at frequencies  $f < f_p$  that are absent in the  $S_{nl}(f)$  estimates. These variations likely are errors caused by reflections from shore. Although reflection is relatively weak in energetic surf zone conditions, the resulting partial standing wave patterns significantly affect wave spectra near the shore where much of the incident wave energy is dissipated (e.g., Guza and Thornton 1982).

#### c. Case III

In the most energetic case III ( $H_s = 3.4$  m,  $f_p = 0.094$  Hz) the entire instrumented transect is well within the surf zone (Figs. 3, 4). The estimates of  $S_{nl}(f)$  and  $F_x(f)$  (Fig. 7) are similar to the case II estimates, with a close balance between energy losses in the energetic part of the spectrum [the negative values of  $F_x(f)$ ] and energy transfers from the spectral peak to higher frequencies [the negative values of  $S_{nl}(f)$ ]. The largest energy transfers occur at stations A–C (Fig. 7), well seaward of the sand bar, causing a factor 2 reduction of the peak spectral level between  $x = 0$  and 160 m (Fig. 3). A similar decay of the second-harmonic peak ( $2f_p = 0.19$  Hz) is observed between  $x = 0$  and 160 m (Fig. 3), but the estimated negative  $F_x(2f_p)$  and positive  $S_{nl}(2f_p)$  do not balance (Fig. 7), suggesting that the second-harmonic energy is dissipated rather than transferred to other parts of the spectrum. Similar to observations in case II, the positive  $S_{nl}$  and nearly zero  $F_x$  estimates at frequencies  $>0.2$  Hz suggest a saturation of spectral levels in the high frequency tail of the spectrum.

No estimates of the energy balance are available at stations D and E on the seaward flank of the sand bar (Fig. 1) owing to an instrument failure. Estimates of  $S_{nl}$  and  $F_x$  at station F on the crest of the sand bar are similar to those obtained at stations A–C (Fig. 7), indicating a continued decay of the spectral peak caused primarily by nonlinear transfers to the saturated high-frequency tail of the spectrum. At stations G and H, located in a trough inshore of the crest of the sand bar (Fig. 1), the  $S_{nl}$  and  $F_x$  estimates indicate a growth of spectral levels in the frequency range 0.1–0.3 Hz at the expense of the spectral peak and higher frequency components (Fig. 7). The approximate balance between  $S_{nl}$  and  $F_x$  suggests that wave breaking and associated dissipation is arrested as waves propagate over the sand bar into slightly deeper water. At station K the estimated nonlinear energy transfers are close to zero. Observations on the shallow beach face (L) show a continued decline of the spectral peak resulting from nonlinear energy transfers to higher frequencies.

In contrast to the strong decay of the spectral peak (about an order of magnitude between the deepest and shallowest instruments), spectral levels at infragravity

frequencies are not attenuated across the surf zone and dominate the spectrum at the shallowest instrument (Fig. 3). Earlier analyses indicate that these infragravity motions are excited predominantly in shallow water by nonlinear triad interactions with incident waves and are trapped near the shore by the sloping beach and shelf [see Herbers et al. (1995) for further discussion]. The resulting standing wave patterns near the shoreline cause large spurious fluctuations of  $F_x(f)$  estimates at sites H, K, and L (Fig. 7). The estimated small nonlinear transfers of energy to infragravity frequencies [ $S_{nl}(f)$  in Fig. 7] also may have significant errors because the effect of standing wave patterns on bispectra and the detuning of triad interactions by directional spreading are neglected (Herbers and Burton 1997; Norheim et al. 1998).

#### d. Case IV

Case IV (Fig. 8) is based on a data record collected a few days after case III when the storm had moved offshore, and moderately energetic swell ( $H_s = 1.6$  m;  $f_p = 0.094$  Hz) propagated across the array. At station A, well seaward of the bar crest, the  $S_{nl}$  and  $F_x$  estimates balance approximately and indicate second-harmonic generation with little or no dissipation. At station B the observed energy transfers are larger, and significant differences between  $S_{nl}$  and  $F_x$  in the range  $0.12 < f < 0.4$  Hz suggest some dissipation, possibly resulting from breaking of the largest waves at the outer edge of the surf zone. No data were collected on the bar crest, but the large reduction in spectral levels between  $x = 110$  and 216 m (Fig. 3) indicates strong dissipation took place owing to intermittent wave breaking on the bar crest. In slightly deeper water shoreward of the sand bar, waves re-formed, and the estimated nonlinear energy transfers are balanced approximately by the energy flux gradients (e.g., stations F–J in Fig. 8). Whereas at station F, energy is transferred primarily from the incident swell peak to the second-harmonic peak (0.19 Hz), the energy transfers are small at station G and reverse sign at stations H–J where the second-harmonic peak is losing energy (i.e., negative values of  $S_{nl}$  and  $F_x$ ) in nonlinear interactions with other parts of the spectrum. Wave breaking on the beach face is evident in large energy losses at stations K and L. Similar to observations of wave breaking farther offshore in cases II and III, the analysis shows that nonlinear interactions transfer energy from the spectral peak ( $S_{nl} \approx F_x < 0$ ) to an apparently saturated high-frequency tail of the spectrum ( $S_{nl} > 0$ ,  $F_x \approx 0$ ), where the energy presumably is dissipated.

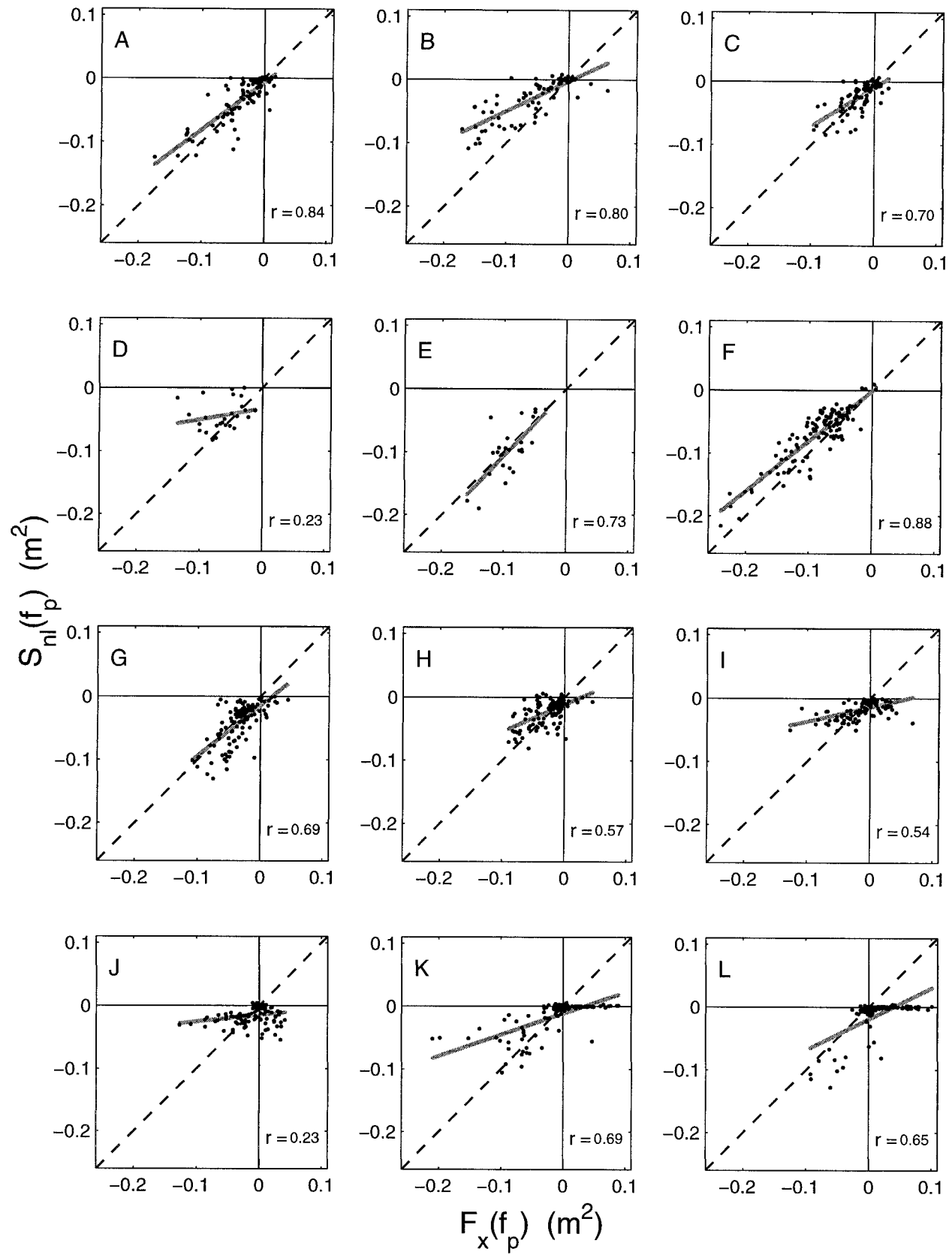
## 4. Discussion

Although the evolution of wave spectra across the beach in the four case studies differs in detail, the characteristics of the observed energy balance in the surf zone are similar with a strong decay of the incident wave spectral peak (Fig. 3) owing primarily to nonlinear energy transfers to higher frequencies (e.g., stations D–H in Fig. 6; A–C, F in Fig. 7; and B, K–L in Fig. 8). This feature of the surf zone energy balance was observed for all energetic events during the two-month-long experiment (Fig. 9). Estimates of  $F_x(f)$  and  $S_{nl}(f)$  at the spectral peak frequency  $f_p$  are compared at all stations for a subset of 125 data records collected when significant wave breaking occurred on the crest of the sand bar (at low tide stages with incident wave heights  $H_s > 1.25$  m). Between station A at the seaward end of the bar crest, the estimated  $S_{nl}(f_p)$  and  $F_x(f_p)$  are both predominantly negative and comparable in magnitude. Linear regression between  $F_x(f_p)$  and  $S_{nl}(f_p)$  estimates at these 8 stations yields best-fit lines within about 5% to 50% of a one-to-one correspondence (Fig. 9). The agreement is particularly good at station F in the vicinity of the bar crest (Fig. 1) where wave breaking often was intense and the largest energy losses were observed. These estimates demonstrate that the strong decay of the spectral peak across the sand bar is primarily the result of nonlinear energy transfers to higher frequencies, rather than direct dissipation of the incident wave components.

The agreement between  $S_{nl}(f_p)$  and  $F_x(f_p)$  estimates is poor at the four stations closest to shore (I–L in Fig. 9). The estimated nonlinear energy transfers are consistently negative and relatively small, whereas corresponding energy flux estimates include large negative and positive values. These estimates may have large errors owing to standing wave patterns (i.e., large differences in spectral levels between nodes and antinodes) in the inner surf zone (Guza and Thornton 1982). In the shallow water WKB approximation an adjacent node and antinode in a standing wave are separated by a quarter wavelength distance  $D = [gh]^{1/2}/(4f)$ . For a water depth  $h = 2$  m and a frequency  $f = 0.1$  Hz,  $D \approx 11$  m, comparable with the separations of sensors used to evaluate energy flux gradients at stations K (10 m) and L (15 m). Thus, partial standing waves may contribute large errors to estimated energy flux gradients that can be either positive or negative depending on the locations of the sensors relative to nodes and antinodes.

Although the present results show that the decay of the spectral peak results primarily from nonlinear energy

FIG. 9. Estimated nonlinear energy transfer  $S_{nl}(f_p)$  vs estimated energy flux gradient  $F_x(f_p)$  at the spectral peak frequency  $f_p$  in energetic surf zone conditions. Each panel shows the comparison at one of the stations A–L (Fig. 1). Each dot represents a 1-h-long data record. Only data records collected within  $\pm 2$  h of low tide with offshore wave variances (measured in 8-m depth)  $> 1000$   $\text{cm}^2$  are included. A linear regression line (solid) and correlation coefficient  $r$  between the  $F_x(f_p)$  and  $S_{nl}(f_p)$  estimates are indicated in each panel. A one-to-one correspondence is indicated with a dashed line.



transfers to higher frequencies, it is less clear what happens subsequently to the transferred energy. In benign conditions with little or no wave breaking, the energy contributes to the growth of second and higher harmonics (case I, Fig. 5). In the moderately energetic case IV (Fig. 8) energy first is transferred to the second-harmonic (station F) and subsequently is transferred to higher frequencies (stations I, J). Observations of wave breaking on the shallow sand bar in case II (Fig. 6, stations F–I) and on the beach face in case IV (Fig. 8, stations K, L) show energy transfers to a broad frequency range that extends to the highest frequency (0.5 Hz) included in the bispectral analysis. These estimates suggest a nonlinear cascade of energy through the high-frequency tail of the spectrum qualitatively similar to the energy balance in deep water wind waves (e.g., Hasselmann et al. 1973; Phillips 1985). However, observations of waves breaking seaward of the sand bar in cases III (Fig. 7, stations A–C) and IV (Fig. 8, station B) show that energy is transferred to, and apparently lost from, a limited ( $\approx 0.15$ – $0.4$  Hz) frequency range. Energy is not exchanged with higher frequencies possibly because at these deeper stations interactions in the high-frequency tail of the spectrum are far from resonance. Triad interactions are near-resonant only for long wavelength components and thus do not allow energy to cascade to length scales that are smaller than the water depth. Other processes neglected in the present analysis, such as turbulent eddy motions and higher-order nonlinear interactions, likely are important in the energy balance of the high-frequency tail of the spectrum (e.g., Battjes 1988, and references therein).

## 5. Summary

The spectral energy balance of shoaling and breaking waves was examined with two months of field observations from a 350-m-long cross-shore transect of 13 pressure sensors deployed on a barred ocean beach near Duck, North Carolina (Elgar et al. 1997). The cross-shore energy flux gradient  $F_x(f)$  was estimated from the measured difference in energy flux between adjacent instruments. The net nonlinear energy transfer  $S_{nl}(f)$  in near-resonant triad interactions was estimated from observed bispectra based on a stochastic formulation of Boussinesq theory (Herbers and Burton 1997).

In low-energy conditions, when waves propagated across the instrumented transect with little or no breaking, the observed small nonlinear energy transfers from the spectral peak to higher frequencies are balanced approximately by the increase in spectral levels at high frequencies, consistent with earlier studies (Freilich and Guza 1984; Elgar and Guza 1985b; Elgar et al. 1997; Norheim et al. 1998). In high-energy conditions when the surf zone extended across the instrumented transect, the  $S_{nl}(f)$  estimates have large negative values in a narrow region near the spectral peak frequency and positive values for a broader range of higher frequencies. The

largest nonlinear energy exchanges were observed on the crest of the sand bar, where wave breaking was most intense. The observed negative  $F_x(f)$  in the energetic part of the spectrum balance approximately the  $S_{nl}(f)$ , indicating that the decay of the spectral peak in the surf zone is caused primarily by nonlinear energy transfers to higher frequencies rather than direct dissipation of the incident wave components. At higher frequencies the observed  $F_x(f)$  are small and do not balance the positive  $S_{nl}(f)$  values, consistent with earlier suggestions (Thornton 1977, 1979) that wave spectra in the surf zone are saturated at high frequencies. That is, energy transferred through nonlinear interactions cannot be absorbed in the high-frequency tail of the spectrum and presumably is dissipated at the rate it is transferred from lower frequencies. The observed balance between energy losses in the energetic part of the spectrum and nonlinear energy transfers to higher frequencies demonstrates that near-resonant triad interactions play a dominant role in the spectral evolution of breaking waves in shallow water.

*Acknowledgments.* This research was supported by the Coastal Dynamics Program of the Office of Naval Research. We thank R. T. Guza, E. L. Gallagher, and B. Raubenheimer for their contributions to the field data collection and the staff of the Scripps Institution of Oceanography Center for Coastal Studies for their tireless efforts to maintain the array for several months. We also thank T. C. Lippmann for providing video images of the surf zone, P. F. Jessen for programming assistance, and E. B. Thornton for helpful discussions. Logistical support and wave data in 8-m depth were provided by the Field Research Facility of the U.S. Army Engineer Waterways Experiment Station's Coastal Engineering Research Center. Permission to use these data is appreciated.

## REFERENCES

- Battjes, J. A., 1988: Surf-zone dynamics. *Annu. Rev. Fluid Mech.*, **20**, 257–293.
- Chen, Y., R. T. Guza, and S. Elgar, 1997: Modeling spectra of breaking surface waves in shallow water. *J. Geophys. Res.*, **102**, 25 035–25 046.
- Eldeberky, Y., and J. A. Battjes, 1996: Spectral modeling of wave breaking: Application to Boussinesq equations. *J. Geophys. Res.*, **101**, 1253–1264.
- Elgar, S., and R. T. Guza, 1985a: Observations of bispectra of shoaling surface gravity waves. *J. Fluid Mech.*, **161**, 425–448.
- , and —, 1985b: Shoaling gravity waves: Comparisons between field observations, linear theory, and a nonlinear model. *J. Fluid Mech.*, **158**, 47–70.
- , T. H. C. Herbers, and R. T. Guza, 1994: Reflection of ocean surface gravity waves from a natural beach. *J. Phys. Oceanogr.*, **24**, 1503–1511.
- , R. T. Guza, B. Raubenheimer, T. H. C. Herbers, and E. L. Gallagher, 1997: Spectral evolution of shoaling and breaking waves on a barred beach. *J. Geophys. Res.*, **102**, 15 797–15 805.
- Freilich, M. H., and R. T. Guza, 1984: Nonlinear effects on shoaling surface gravity waves. *Philos. Trans. Roy. Soc. London*, **A311**, 1–41.

- Gallagher, E. L., S. Elgar, and R. T. Guza, 1998: Observations of sand bar evolution on a natural beach. *J. Geophys. Res.*, **103**, 3203–3215.
- Guza, R. T., and E. B. Thornton, 1982: Swash oscillations on a natural beach. *J. Geophys. Res.*, **87**, 483–491.
- Hasselmann, K., and Coauthors, 1973: Measurements of wind wave growth and swell decay during the Joint North Sea Wave Project (JONSWAP). *Dtsch. Hydrogr. Z.*, **A8** (Suppl.), 5–95.
- Herbers, T. H. C., and M. C. Burton, 1997: Nonlinear shoaling of directionally spread waves on a beach. *J. Geophys. Res.*, **102**, 21 101–21 114.
- , S. Elgar, and R. T. Guza, 1994: Infragravity-frequency (0.005–0.05 Hz) motions on the shelf. Part I: Forced waves. *J. Phys. Oceanogr.*, **24**, 917–927.
- , —, and —, 1995: Generation and propagation of infragravity waves. *J. Geophys. Res.*, **100**, 24 863–24 872.
- Kaihatu, J. M., and J. T. Kirby, 1995: Nonlinear transformation of waves in finite water depth. *Phys. Fluids*, **7**, 1903–1914.
- Kinsman, B., 1965: *Wind Waves: Their Generation and Propagation on the Ocean Surface*. Prentice-Hall, 676 pp.
- Mase, H., and J. T. Kirby, 1992: Hybrid frequency-domain KdV equation for random wave transformation. *Proc. 23d Int. Conf. Coastal Eng.*, Venice, Italy, ASCE, 474–487.
- Norheim, C. A., T. H. C. Herbers, and S. Elgar, 1998: Nonlinear evolution of surface wave spectra on a beach. *J. Phys. Oceanogr.*, **28**, 1534–1551.
- Peregrine, D. H., 1967: Long waves on a beach. *J. Fluid Mech.*, **27**, 815–827.
- Phillips, O. M., 1985: Spectral and statistical properties of the equilibrium range in wind-generated gravity waves. *J. Fluid Mech.*, **156**, 505–531.
- Smith, J. M., and C. L. Vincent, 1992: Shoaling and decay of two wave trains on a beach. *J. Waterway Port Coastal Ocean Eng.*, **118**, 517–533.
- Thornton, E. B., 1977: Rederivation of the saturation range in the frequency spectrum of wind-generated gravity waves. *J. Phys. Oceanogr.*, **7**, 137–140.
- , 1979: Energetics of breaking waves within the surf zone. *J. Geophys. Res.*, **84**, 4931–4938.